The dynamics and geometry of a two-dimensional turbulent front

Ruo-Shan Tseng[a] and Tony Maxworthy[b]
Department of Aerospace Engineering, University of Southern California, Los Angeles, California 90089-1191

(Received 14 April 1989; accepted 19 March 1990)

The formation and evolution of a front between turbulent and nonturbulent fluid in a two-dimensional flow are studied using a combined experimental-numerical technique. Turbulence was created by towing a grid of vertical bars partway through a tank that was filled with a two-layer stratified fluid. The velocity field at several times during the evolution of the turbulence was obtained by photographing neutrally buoyant particles suspended in the sharp density interface. Each realization was used to compute the advance of lines of particles released in the flow near the initial location of the grid. The computed location and shape of the turbulent/nonturbulent front, representing the distribution of a passive scalar in the flow, correlate well with the "zero contour" of the absolute-vorticity field. It is shown that the turbulent/nonturbulent front, in the most distorted cases, may be described by a fractal dimension over a restricted range of length scales. Certain geometric characteristics of the frontal region, in particular the probability distribution of a passive scalar, the frontal width, and length are also examined; the latter appears to grow with a power of time related to the fractal dimension of the interface.

I. INTRODUCTION

The problem of mixing and the subsequent collapse of turbulent structures under the influence of a gravitational restoring force has been of great interest to fluid dynamicists, oceanographers, and meteorologists for many years. This interest is motivated primarily by its practical application of estimating the vertical transport of heat and mass in the ocean and the atmosphere. There have been a relatively large number of grid-turbulence experiments in stratified fluid with horizontally inhomogeneous configurations.[1-6] It was clearly demonstrated in these experiments that vertical scales in the turbulent field are limited by stable stratification, the vertical interface or front between turbulent and nonturbulent fluid collapses into a series of intrusive layers, while farther from the grid the motion is dominated by internal waves. Among the aforementioned experiments, Liu *et al.*,[5] for the first time, reported the appearance of three-dimensional motions sometime after the initial collapse of basically two-dimensional intrusions. They observed that initially the intrusions can evolve freely in both horizontal directions so that the flattened horizontal eddies that are formed are not constrained by side walls and can develop gradually from smaller to larger scales. The structure of the collapsed state of turbulence (internal waves and/or quasi-two-dimensional turbulence) is of considerable importance to the interpretation of oceanographic measurements.[6] We believe that three-dimensional effects are crucially important in deciding both the scale and subsequent motions of these intrusions and should deserve more attention. The present experiment, therefore, was devised to investigate the formation and evolution of a front in a tank of relatively large horizontal extent (therefore the long-time evolution of eddies to very large scales can be studied) and in a simple two-dimensional turbulent flow with vertical vortices. We produced a front at the sharp density interface of a two-layer system with the stratification to suppress vertical motions and investigated its characteristics using particle tracking methods.

II. APPARATUS AND PROCEDURE

The experiments were performed in a square tank (240×240 cm) that was filled with a two-layer stratified fluid of 14 cm total depth (Fig. 1). This two-layer system consisted mainly of an upper layer of fresh water lying over salt water of density 1.040 g/cm^3; both layers were of the same depth of 6.5 cm. A thin layer of salt-saturated water, 1 cm deep, was introduced beneath this two-layer fluid in order to reduce the interaction of vorticities with the bottom of the tank. A large number of polystyrene particles, which are commercially available with an intermediate density, and of dimensions $3.5\times3.0\times2.0$ mm, were placed in the fresh–salt water interface to mark the flow field. Turbulence was created by towing a grid of vertical bars 3 cm wide, set on 15 cm centers through the depth of the fluid from midway along one side to the end of the tank. The grid was towed at a constant speed of 5 cm/sec, which is fast enough to produce a considerable intensity of turbulence, yet slow enough to prevent the generation of unwanted internal waves that might introduce more complication. In this way a horizontal, two-dimensional front was generated after a short transient period of three-dimensional turbulent motion. The evolution of this quasi-two-dimensional turbulent flow, over a large time scale, was visualized by photographing the neutrally buoyant particles from the top of the tank with time exposures between 4 and 13 sec. The particle streaks were then digitized, and the resulting velocities interpolated onto a regular 32×32 grid for further analysis.

[a] Present address: Rosenstiel School of Marine and Atmospheric Science, University of Miami, Miami, Florida 33149.
[b] Also, Department of Mechanical Engineering.

 0899-8213/90/071224-07$02.00

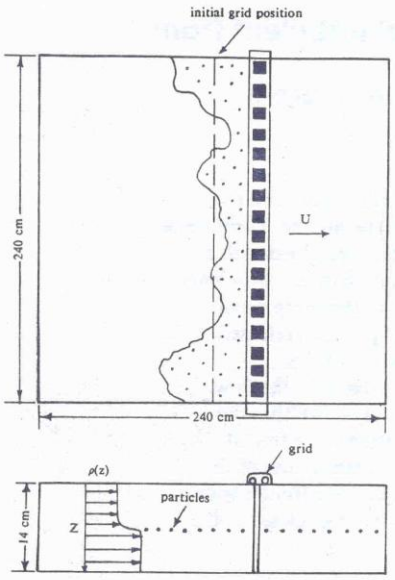

FIG. 1. Apparatus.

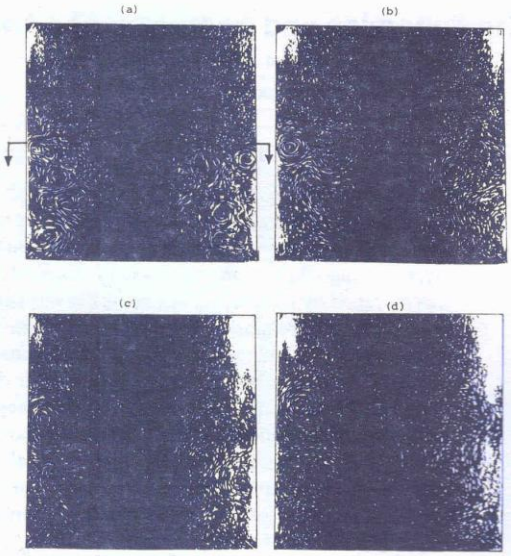

FIG. 2. Streak photographs of the evolution of the turbulent/nonturbulent front. Photographs were taken at (a) 30, (b) 129, (c) 238, and (d) 393 sec after the beginning of the grid motion. The arrows indicate the direction of the grid motion.

III. RESULTS

A. Qualitative description of the flow field

A sequence of streak photographs of the evolutionary process at four different times is shown in Fig. 2. After the passage of the grid, a short transient period of three-dimensional turbulent motion was first generated; this three-dimensional turbulent motion was inhibited vertically by the stratification at the layer of fresh–salt water interface and it quickly became quasi-two-dimensional. At the earliest time, some 30 sec after the beginning of grid motion [Fig. 2(a)], a large number of vortices with irregular size, shape, and intensity could be observed in the turbulent field; the boundary between turbulent zone and quiescent region, i.e., the front, was well defined and was still near the middle of the whole domain. As time progressed the vortices at both edges of the tank were advected by the mean flow toward the tranquil region, while the nonturbulent fluid at the central portion was entrained into the turbulent field. As a result of this mixing process the front started to grow and became distorted. The process of vortex merging was seen to be taking place in the turbulent region when two vortices were of the same sign and were close enough. This process has been widely studied because of its dominant role in the reverse energy transfer that produces large structures in evolving two-dimensional turbulence.[7–9] At the latest time, about 400 sec [Fig. 2(d)], the two-dimensional motion was still quite intense, the vortices developed to a considerable size, and the front was quite distorted.

B. Vorticity field

It is generally understood that the front between turbulent and nonturbulent fluid means the interface separating vortical and nonvortical regions of the flow. The interpolated velocity field was differentiated to obtain contours of the absolute value of vorticity, $|\omega|$. This field is illustrated in Fig. 3 at four different times to distinguish the quiescent region from the turbulent field regardless of the sign of vorticity. In this way the contour line of the smallest value of $|\omega|$ can be considered as one measure of the location of the front. However, the usefulness of this determination is difficult to ascertain in view of our inability to calculate such small values of $|\omega|$ with sufficient accuracy. In Fig. 3(a) (at early time $t = 30$ sec) we can see that the front defined in this way, comprised the outer edges of a large number of small vortices and that it was still near the center of the tank. As the front continued to evolve many of these small vortices amalgamated together so that the final stages [Fig. 3(d)] were dominated by the growth of only a few large vortices.

C. Length scales and energy spectrum of turbulent field

The turbulence integral scale (ℓ) and Kolmogorov scale (η) of the turbulent field from our results at different times were calculated using standard techniques[10] and are listed in Table I. That is, the integral scale was obtained from correlation measurements and the Kolmogorov scale was calculated from $\eta = (\nu^3/\epsilon)^{1/4}$, where ν is the kinematic viscosity, ϵ is the energy dissipation rate defined as $\epsilon = u'^3/\ell$, and u' is the rms horizontal velocity fluctuations. As we have discussed in the previous section, the characteristic length scales of the turbulent field were seen to increase as time progressed simply by visual inspection of the streak photo-

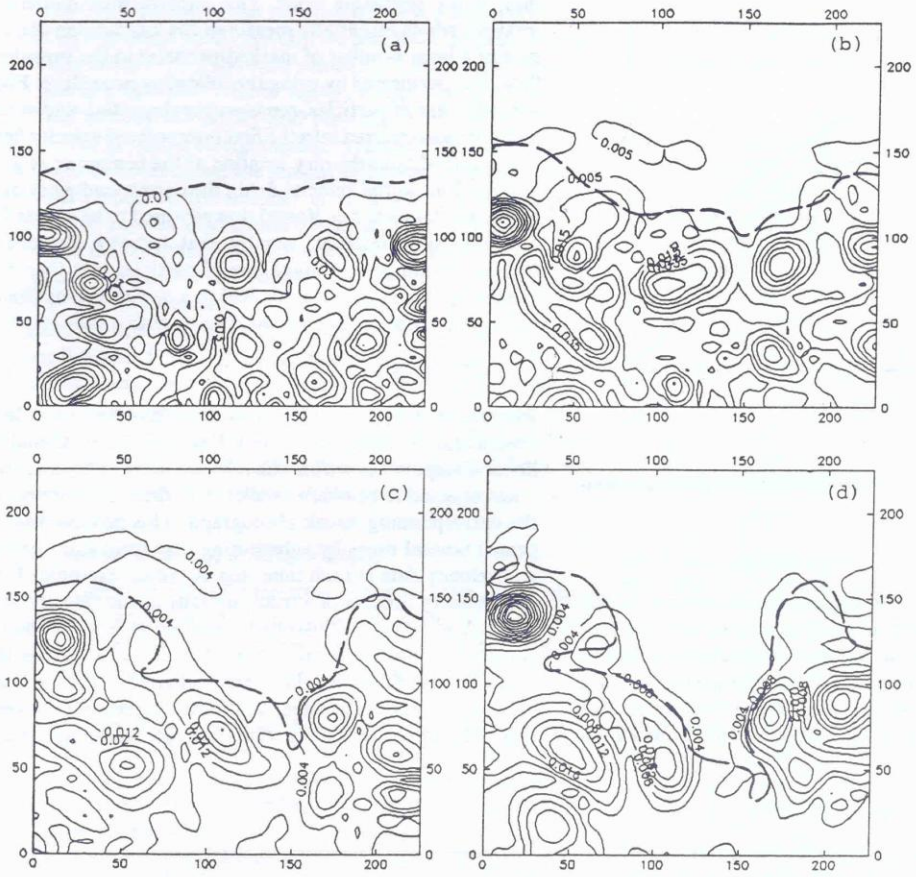

FIG. 3. Contour of $|\omega|$ with calculated front location (broken curves) superimposed at (a) 30, (b) 129, (c) 238, (d) 393 sec after the start of grid motion.

graphs. This observation is borne out by the quantitative measurements listed in Table I.

Previous studies of two-dimensional turbulence were performed in the same tank as this study under similar conditions except with a linearly stratified fluid and in the absence of a front.[8] Presumably the inertia-range transfers of energy and enstrophy (mean-square vorticity) of two-dimensional turbulence in our experiment should be similar in form to those found in the absence of the front. The energy spectrum $E(k)$, calculated directly from the kinetic energy field from their measurements,[8] is shown in Fig. 4 for three different times. It is seen in this figure that the energy spectrum in the enstrophy cascading range followed the form $E(k) \approx k^{-\alpha}$, where k is the horizontal wave number; the value of the spectral slope at small k is greater than the k^{-3} law derived from inviscid similarity theories, and of the same magnitude or even smaller than the k^{-4} law found in numerical experiments.[9,11]

TABLE I. Calculated turbulence length scales.

Time (sec)	ℓ (cm)	η (cm)
30.8	7.1	0.070
52.9	10.2	0.104
89.0	12.9	0.138
128.9	15.6	0.145
172.8	16.2	0.213
238.2	18.1	0.205
311.5	19.2	0.267
393.2	20.7	0.278

IV. A COMBINED EXPERIMENTAL-NUMERICAL COMPUTATION

In principle the evolution of the turbulent front could have been obtained by monitoring a horizontal dye streak set in the center of the tank at the initial location of the grid. However, from a number of preliminary experiments we

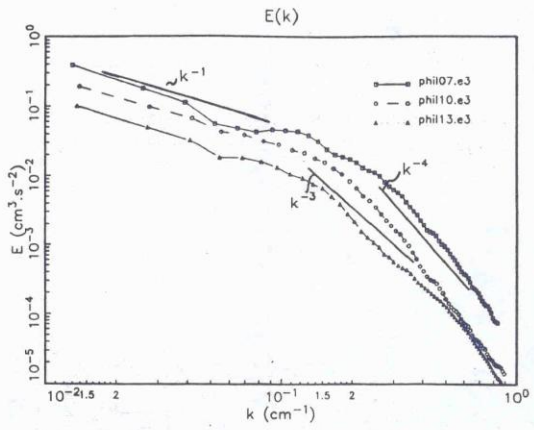

FIG. 4. Energy spectrum of two-dimensional turbulence obtained by Maxworthy *et al.*[8]

found that it was difficult to perform an experiment of this type because the dye became easily entrained into the near wake of the grid bars when the dye was released too close to the initial position of the grid. As an alternative we have devised a scheme that uses the measured velocity data in a step-by-step numerical calculation to determine the evolution of the turbulent front. This experimental-numerical method, which essentially measured the Lagrangian dispersion of a large number of marked particles in the turbulent flow, was performed by using the following procedure. First a straight line of particles, representing the initial, undistorted front, was inserted into the first interpolated velocity field at a specified but arbitrary location at the beginning of grid motion. This initial velocity field (the corresponding photograph was taken at $t = 30$ sec) was assumed to be frozen for a certain time interval, usually that between successive frames; the initially straight line of particles was then advanced by the frozen velocity field to a new shape and location using a first-order forward scheme with a time step τ,

$$x(t+\tau) = x(t) + \tau V(x(t),t), \tag{1}$$

where $x(t)$ and $x(t+\tau)$ are positions of a certain particle at times t and $t+\tau$ and the velocity V at $x(t)$ was evaluated by linear interpolation within the relevant mesh. The time step τ was selected to be much smaller than the exposure time of the corresponding streak photograph. This process was repeated several times by substituting new front information and velocity data at each time step. A typical example of the evolutionary process of a front, initially at the velocity-grid position $y_0 = 19$, is illustrated together with the vorticity contours at four different times (Fig. 3). Comparing the distorted interface with the "zero" contour of the vorticity field, we see the reasonable, qualitative agreement between them. It is important to note that the major advantage of this

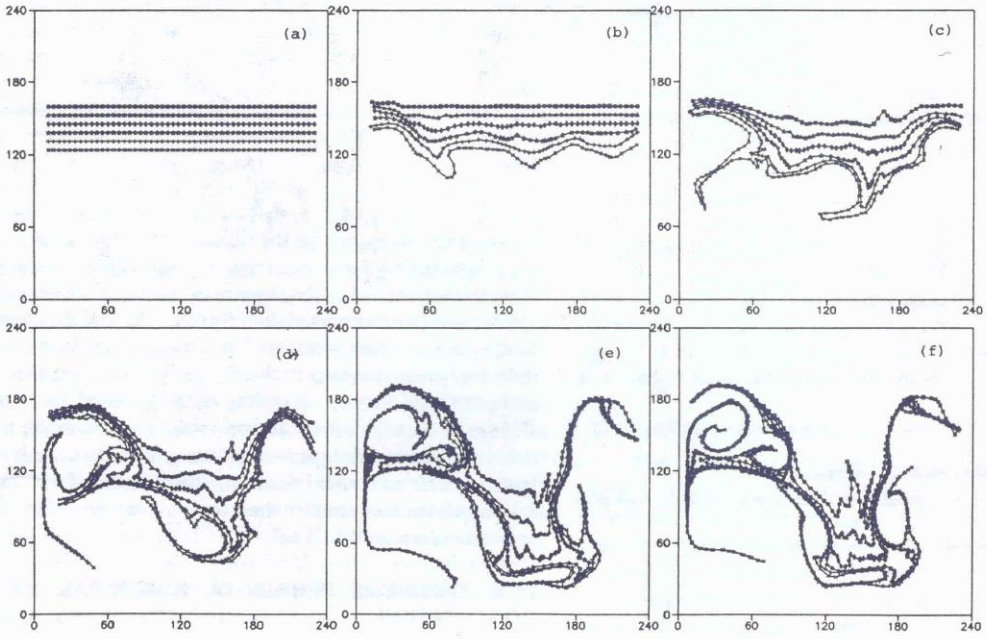

FIG. 5. Evolution of a passive frontal region at (a) 0, (b) 40, (c) 150, (d) 280, (e) and (f) 500 sec after the start of grid motion.

numerical method is that the evolution of any arbitrary front at any specified initial position we desire can be determined. Figures 5(a)–5(e) show the numerical results for the evolution of a turbulent frontal region, comprising six interface lines initially at velocity-grid positions $y_0 = 17$, 18, 19, 20, 21, and 22, based on eight different realizations and 160 time steps. In order to test the sensitivity of the numerical results with respect to the number of realizations used, we performed another calculation based on four different realizations; the resultant front at $t = 500$ sec is shown in Fig. 5(f). It can be seen that the shape and location of particle lines at $t = 500$ sec determined from eight realizations [Fig. 5(e)] does not differ significantly from those determined from four realizations [Fig. 5(f)], and that good accuracy can be assured using the former calculations [Fig. 5(e)]. Based on this technique we are able to model the distribution of a passive scalar (e.g., temperature or salinity) of a front and then find some way to characterize this distorted front, as discussed in the following sections.

A. Measurement of interface width

One of the more interesting characteristics of the processes shown in Fig. 5 is a measure of the width of the front in the y direction, which is important because of its practical implications concerning the long-time behavior of real fronts in the ocean and the atmosphere.

There have been some related studies of the interface growth in a Hele–Shaw cell,[12–14] and we have used these results in an attempt to describe the complex structures of fronts. Following Maxworthy,[14] we have defined the density distribution $\rho(y)$ and the interface width (δ) as sketched in Fig. 6. For any particular initial realization of a turbulent front, consisting of n evenly spaced lines [e.g., Fig. 5(a)], we assume that the fluid in the region $y < y_1$ has an assigned weight of $\rho_i = 1$ and the region $y > y_n$ has an assigned weight of $\rho_i = 0$ with a suitable distribution of weights in between, then the density $\rho(y)$ can be defined as

$$\rho(y) = \sum \frac{L_i \rho_i}{W}, \tag{2}$$

where L_i and ρ_i are, respectively, the sum of the length of the straight horizontal lines and the weight of some convected scalar attached to the fluid located in the region between interface lines i and $i-1$ at any specific value of y, and W is the width of the tank. This process was repeated for many values of y. As pointed out earlier by Maxworthy,[14] $\rho(y)$ can be considered as a measure of the "scalar density" distribution within the front or alternatively the probability of being located in one type of fluid at any particular value of y. Plots of ρ against y at different times are given in Fig. 7. The scalar density of the fluid located at the upper half of the tank does not change very much at early times, but increases rather rapidly as time progresses. Also of interest is the rise in the proportion of fluid with ρ_i close to one at larger values of y at the latest time ($t = 500$ sec), a result which is similar to the findings of Maxworthy[14] although the mechanisms involved are quite different in both cases. Here this effect is apparently due to the gradual formation of a strong eddy near the left, upper corner of the field [Fig. 2(d)].

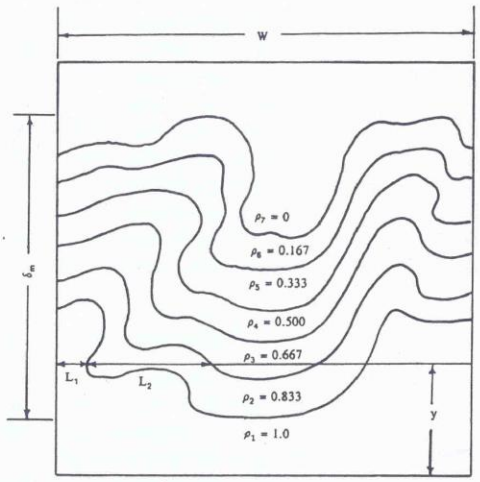

FIG. 6. Definition of the density distribution $\rho(y) = \Sigma_{i=1}^{n} L_i \rho_i / W$, and the front width $\delta = \int_{-\infty}^{\infty} \rho(y)[1-\rho(y)]dy$.

The interface width (δ) as defined here is based on a concept similar to the momentum thickness of boundary layer theory,[15] i.e.,

$$\delta = \int_{-\infty}^{\infty} \rho(y)[1-\rho(y)]dy. \tag{3}$$

Plotted in Fig. 8 is the interface width calculated from (3) at different times. The interface width was found to increase fairly linearly with respect to time at the larger times, and to increase less rapidly at earlier times. Another measure of the front width is δ_m, defined as the total maximum width between the extreme ends of the distorted front (Fig. 6). The maximum width, plotted in Fig. 9, demonstrates a similar trend of linear growth with time at longer times, as that of Fig. 8. The results of Maxworthy[14] also indicated that the

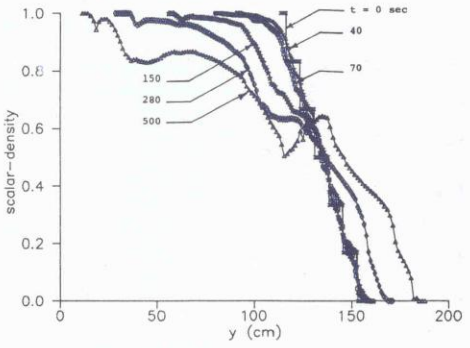

FIG. 7. Density distribution ρ vs y for different times. The front consists of six interface lines with the values of ρ_i given in Fig. 6.

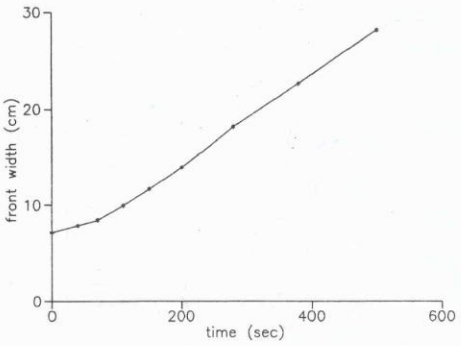

FIG. 8. Front width δ versus time t.

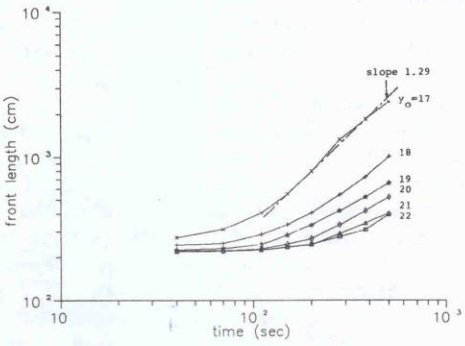

FIG. 10. Front length L versus time t for different initial front locations.

interface width in a Hele–Shaw cell grows linearly with time at large times.

B. Measure of interface distortion—Interface length and fractal dimension

The interface length (L) for six different initial front locations was obtained and is plotted in Fig. 10 versus time. For the case of $y_0 = 17$, the interface length is seen to be much larger than that of the other cases. This indicates that the front was much more contorted near the turbulent/nonturbulent boundary than farther away.

As suggested by Mandelbrodt[16] and verified by many others, one possible way to characterize the distortion of an interface is to measure its fractal dimension. The fractal dimension (d) of a distorted interface can be found by the following relationship:

$$N \approx G^{-d} \quad \text{or} \quad L_G = NG \approx G^{1-d}, \tag{4}$$

where L_G is the length of the interface when measured by a "ruler" or "gauge" of length G, and N is the number of steps required to fit the interface. For an ordinary, one-dimensional curve, d has the value of unity; but for a fractal curve, d has a value between 1 and 2. We have plotted logarithmically the interface length of Fig. 5 at various times and initial locations versus the gauge length, and the fractal dimension is $(1 + n)$ if the resultant line has a constant-negative slope of $(-n)$. It is shown in Fig. 11 that only for cases of more distorted interface lines do the curves of L_G vs G yield a limited region of constant-negative slope for values of G from about 15 to 45 cm. Note that the lower end of the constant-negative slope region is about 50 times the Kolmogorov scale, and the high cutoff seems to occur around two or three times the integral scale of turbulence. The fractal dimension for the cases of more distorted fronts is found to have an average value of about 1.29. For the other cases at short times of which the fronts are not so contorted, the existence of a fractal dimension is more doubtful. The signifi-

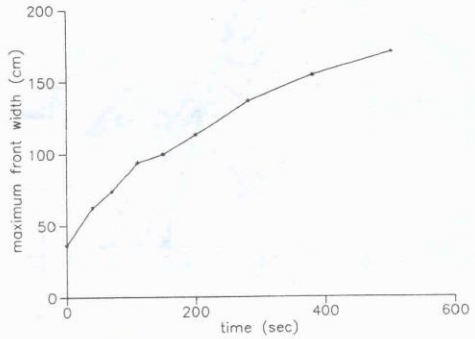

FIG. 9. Maximum front width δ_m versus time t.

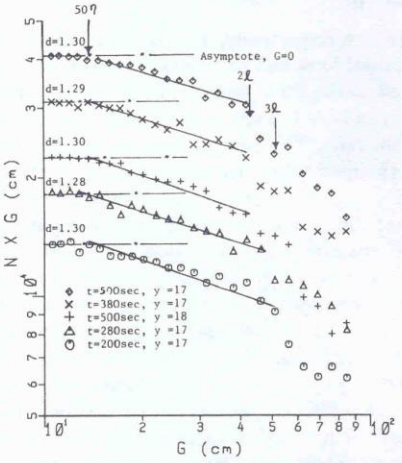

FIG. 11. Interface length as measured with a certain gauge length G versus the value of G itself, for some cases.

cance of the fractal dimension is that it has a possible relationship to the interface evolution, in particular, the power of time at which the interface length grows at longer times may have a value close to that of the dimension.[14] This relationship is also well supported by the present result for the case of the most distorted interface line, $y_0 = 17$ (Fig. 10).

It was pointed out by Sreenivasan and Meneveau[17] and by Turcotte[18] that the turbulent/nonturbulent interface may possess fractal-like behavior and that its fractal dimension can be measured. Based on their experimental data and the method of two-dimensional or one-dimensional slicing, Sreenivasan and Meneveau concluded that the fractal dimension of the turbulent/nonturbulent interface in several classical turbulent flows (boundary layer, axisymmetric jet, and plane wake) ranged from 1.32 to 1.40. They also found that there is a sizable constant-slope region between η and 3ℓ, which is consistent with the concept of scale similarity that fully developed turbulence consists of a hierarchy of eddies, or scales of various size of the order between the Kolmogorov scale and integral scale of motion. We should emphasize that in our case, in order to detect similarity on scales of the order of η, the particle spacing must be substantially smaller than that used here. This condition was not fulfilled in the present study because of the limitation of computer capacity and therefore explains why the lower bound of scale similarity in our results is considerably greater than the Kolmogorov scale. We will focus on these discrepancies in our future work.

V. CONCLUSIONS

The present work has examined experimentally the long-time evolution of horizontal eddies and the formation and distortion of a front between turbulent and nonturbulent fluid in a simple two-layer stratified flow. Streak photographs clearly showed that in this flow the intrusions can evolve freely in both horizontal directions and the eddies that are formed can evolve from smaller to larger horizontal scales. Calculated results of the energy spectrum and length scales of the turbulent field are largely in accord with the predictions of two-dimensional turbulence theories and thus point out that such a theory is helpful in describing the evolution of similar flow in the ocean and the atmosphere.

Quantitative descriptions of the turbulent/nonturbulent front or equivalently, the distribution of a passive scalar in the flow was provided by using a combined experimental-numerical technique. Comparisons between the computed location and shape of the front and the "zero contour" of the absolute-vorticity field show good agreements, and therefore support the accuracy of this technique. The front width was found to increase rather linearly with respect to time at longer times. Finally, one of the most important conclusions of the present work is that the turbulent/nonturbulent front, in the most distorted cases, can be described by self-similar fractals over a restricted range of scales. We found that the power of time at which the interface length grows at larger times may have a value very close to that of the fractal dimension.

ACKNOWLEDGMENTS

The assistance of Dr. G. R. Spedding in setting up the programming on which much of this work is based is gratefully acknowledged.

The support of this research by the Office of Naval Research, Physical Oceanography and Fluid Dynamics Programs (Contract No. N00014-82-K-0084), is also gratefully acknowledged.

[1] T. D. Dicky and G. L. Mellor, J. Fluid Mech. **99**, 13 (1980).
[2] S. A. Thorpe, J. Fluid Mech. **124**, 391 (1982).
[3] G. C. Ivey and G. M. Corcos, J. Fluid Mech. **121**, 1 (1982).
[4] F. K. Browand and E. J. Hopfinger, in *Turbulence and Diffusion in Stable Environment* (Oxford U. P., Oxford, England, 1986), p. 15.
[5] Y. N. Liu, T. Maxworthy, and G. R. Spedding, J. Geophys. Res. **92**, 5427 (1987).
[6] E. J. Hopfinger, J. Geophys. Res. **92**, 5287 (1987).
[7] Y. Couder and C. Basdevant, J. Fluid Mech. **173**, 225 (1986).
[8] T. Maxworthy, P. Caperan, and G. R. Spedding, Third International Symposium on Stratified Flow, Pasadena, California, 1987. Preprint.
[9] J. C. McWilliams, J. Fluid Mech. **146**, 21 (1984).
[10] H. Tennekes and J. L. Lumley, *A First Course in Turbulence* (MIT U.P., Cambridge, MA, 1972).
[11] P. B. Rhines, Annu. Rev. Fluid Mech. **11**, 401 (1979).
[12] P. G. Saffman and G. I. Taylor, Proc. R. Soc. London Ser. A **245**, 312 (1958).
[13] J. Nittman, G. Daccord, and H. E. Stanley, Nature **314**, 141 (1985).
[14] T. Maxworthy, J. Fluid Mech. **177**, 207 (1987).
[15] H. Schlichting, *Boundary-Layer Theory* (McGraw-Hill, New York, 1979), 7th ed.
[16] B. Mandelbrodt, *The Fractal Geometry of Nature* (Freeman, San Francisco, 1983).
[17] K. R. Sreenivasan and C. Meneveau, J. Fluid Mech. **173**, 357 (1986).
[18] D. L. Turcotte, Annu. Rev. Fluid Mech. **20**, 5 (1988).